Alexandria Engineering Journal (2021) 60, 5485–5494

HOSTED BY

ELSEVIER

Alexandria University

Alexandria Engineering Journal

www.elsevier.com/locate/aej
www.sciencedirect.com

A novel method of model predictive control on permanent magnet synchronous machine with Laguerre functions

Lihua Gao [a,b], **Guangming Zhang** [a,*], **Huiminou Yang** [a], **Lei Mei** [a]

[a] *School of Mechanical and Power Engineering, Nanjing Tech University, Nanjing 211816, China*
[b] *Nanjing Polytechnic Institute, Nanjing 210048, China*

Received 11 December 2020; revised 2 March 2021; accepted 20 March 2021
Available online 5 June 2021

KEYWORDS

Permanent magnet synchronous machine (PMSM);
model predictive control (MPC);
Laguerre functions;
Constraints

Abstract This paper aims to speed up the response and alleviate the computing load of model predictive control (MPC) of permanent magnet synchronous machine (PMSM). For this purpose, the Laguerre functions were extended to MPC, creating novel linear controller (LMPC) for the PMSM model. Firstly, the differences of control variables between adjacent sampling periods were regarded as a unit impulse response of a stable system, which can be approximated by a few terms of Laguerre polynomials. In this way, the difference of control variables can converge to zero quickly through parameter adjustment. Then, the current and voltage constraints in the form of Laguerre functions were applied on PMSM to improve the current response to sudden changes of speed or load. Furthermore, the torque load was applied to the state space model of PMSM to optimize the response to external load. Simulation results show that the proposed LMPC controller can effectively reduce the computing complexity that restricts the application of MPC on PMSM.

1. Introduction

Recently, the permanent magnet synchronous machine (PMSM)has been widely used in electric vehicles (EVs), owing to its high power density, large torque, and excellent efficiency [1–6]. To adapt to the high performance, new or improved algorithms must be designed for the control of PMSM.

There are many approaches for PMSM control [7,8]. As a classical approach, field-oriented control (FOC) integrates multiple proportional-integral (PI) controllers, namely, speed loop, current loop, and torque loop [9–11]. Since each control loop runs independently, it is impossible to implement the control from the global perspective. Besides, the current and voltage constraints cannot be applied to all loops at once, causing the current to soar during the initial, speed-change, or load-change processes. Furthermore, the uncertain factors (e.g., nonlinearity, time-varying parameters, and interference of load

* Corresponding author.
E-mail address: zgm@njtech.edu.cn (G. Zhang).

☆ This work was supported in part by the National Natural Science Foundation of ChinaunderGrant61703202, in part by the Key Research Development Project of Jiangsu Province under Grant BE2017164, and in part by the Key Research Development Project of Nanjing Polytechnic Institute under Grant NHKY-2020-08.
Peer review under responsibility of Faculty of Engineering, Alexandria University.

https://doi.org/10.1016/j.aej.2021.03.035

torque) make it difficult to automatically adjust the parameters of PI controllers.

Model predictive control (MPC) is a conventional strategy in control engineering. In recent years, MPC has been introduced to industrial control, thanks to its various advantages [12–15]: First, discrete MPC can effectively deal with multivariable systems based on the state space model, including both single-input single-output (SISO)system and multi-input multi-output (MIMO) system. Second, MPC can simultaneously process the constraints of state, control, and output variables in multivariable systems. Third, MPC supports the optimal control of constraints and global control of the target, without needing the extra controllers as FOC [16–20]. In general, MPC is implemented in three steps: predictive model, receding horizon control and feedback control. If applied to PMSM, MPC will derive a cost function from the PMSM model and parameters in each sampling period, and use the function to optimize the control variables of the system [21,22].

With the development of hardware, MPC has now been adopted for high sampling, fast PMSM. For example, Liu et al. [7] and Mynar et al. [8] relied on the explicit MPC to optimize the control variables of PMSM, and successfully improved the predictive effect and receding horizon level; but the success is achieved with a rising workload of seeking the optimal region. Preindl and Bolognani [23] realized model predictive direct torque control, using finite control set (FCS). Some MPC algorithms are directly rooted in multiparametric quadratic program, featuring offline calculation and online update of optimal control variables. For instance, Bolognani et al. [24] incorporated the multiparametric quadratic program into MPC to optimize the control variables through binary search, speeded up the execution of MPC algorithm, and completed the computation offline.

This paper details the application of Laguerre functions in MPC for PMSM. These functions have been extensively used for signal analysis, parameter identification [25], and recently for MPC [26]. The main contributions are as follows:

(1) In order to predict the results more accurately, the MPC predictive period is usually longer, so the computation of MPC is large. In order to reduce the predictive period number of MPC, Laguerre functions were introduced to MPC. By adjusting the parameters of Laguerre function, to reduce the period of predictive. Meanwhile, the current and voltage constraints in the form of Laguerre functions were applied on PMSM to improve the current response to sudden changes of speed or load.
(2) A novel state space model was used for LMPC: the torque load was applied to the state space model of PMSM to optimize the response to external load.

The remainder of this paper is organized as follows: Section 1 introduces the basic theories on MPC and PMSM model; Section 3 implements PMSM control based on LMPC; Section 4 presents the simulation results; Section 5 puts forward the conclusions.

2. Method

2.1. PMSM model

In the dq0 rotating reference frame, the continuous-time electrical dynamics equations of a PMSM can be described by:

$$\begin{aligned}\frac{di_d}{dt} &= -\frac{R_s}{L_d}i_d + \frac{L_q}{L_d}P\omega_m i_q + \frac{u_d}{L_d}\\ \frac{di_q}{dt} &= -\frac{L_d}{L_q}P\omega_m i_d - \frac{R_s}{L_q}i_q - \frac{\phi_f}{L_q}P\omega_m + \frac{u_q}{L_q}\\ \frac{d\omega_m}{dt} &= \frac{1}{J}(1.5P\phi_f i_q + (L_d - L_q)i_d i_q) - B\omega_m - T_l\end{aligned} \tag{1}$$

The electromagnetic differential equation can be expressed as:

$$Te = \frac{3}{2}P[\phi_f i_q + (L_d - L_q)i_d i_q] \tag{2}$$

The mechanical dynamic differential equations can be described by:

$$\begin{aligned}\frac{d\omega_m}{dt} &= -\frac{f}{J}\omega_m + \frac{1}{J}Te - \frac{1}{J}T_l\\ \frac{d\theta_m}{dt} &= \omega_m\\ \frac{dT_l}{dt} &= 0\end{aligned} \tag{3}$$

where, ω_m is the mechanical angular speed of rotor; θ_m is the position of rotator; f is the friction coefficient; J is the moment of inertia; T_l is the load torque; ϕ_f is the electromotive force constant; R_s is the stator winding resistance; L_d is the stator inductance component of axis d; L_q is the stator inductance componentof axis q; P is the number of pole pairs; u_d is the stator voltage component of axis d; u_q is the stator voltage component of axis q; i_d is the stator current component of axis d; i_q is the stator current componentof axis q; T_e is the electromagnetic torque.

To design a discrete MPC controller, the PMSM system must be discretized in advance. Thus, formula (1) can be converted into a set of formulas:

$$\begin{aligned}i_d(k+1) &= \tfrac{L_d - TR_s}{L_d}i_d(k) + TP\tfrac{L_q}{L_d}\omega_m i_q(k) + \tfrac{T}{L_d}u_d(k)\\ i_q(k+1) &= \tfrac{L_q - TR_s}{Lq}i_q(k) - TP\tfrac{L_d}{L_q}\omega_m i_d(k)\\ &\quad - TP\tfrac{\phi_f}{L_q}\omega_m(k) + \tfrac{T}{L_q}u_q(k)\\ \omega_m(k+1) &= \omega_m(k) + \tfrac{T}{J}(\tfrac{3}{2}[\phi_f i_q(k) + (L_d - L_q)i_d i_q(k)])\\ &\quad - \tfrac{T}{J}T_l(k)\end{aligned} \tag{4}$$

It is well known that MPC must be implemented in a linear system. However, there are nonlinear coupling terms in formula (4): $\omega_m i_d(k), \omega_m i_q(k), i_d i_q(k)$. Bolognani et al. [24] provided three approaches for removing these nonlinear terms: If the PMSM is surface mounted with null or low saliency, i.e. $L_d = L_q$, the third formula of set (4) naturally becomes linear; if the PMSM is an interior system with different inductances on axes d and q, the nonlinear terms can be considered as measurement disturbances, and added to the state model; the rotor speed can be assumed to be constant $\omega_m = \Omega$ to eliminate nonlinear mathematical operations.

This paper selects the second approach to linearize the PMSM system. $\omega_m i_d(k), \omega_m i_q(k), i_d i_q(k)$ were deemed as measurement disturbances updated by $i_d(k), i_q(k), \omega_m(k)$, which can be measured in each sampling period. In this way, the formulas in set (4) were linearized. However, parameter T_l cannot be adjusted or generated by PMSM, but assigned by the user. Here, an extended Kalman filter (EKF) observer is introduced to estimate T_l based on the model (3). The load torque can be observed precisely based on the measured mechanical position θ_m. Thus, all obstacles in the application of MPC in PMSM model have been removed. Then, the state variables can be selected as:

$$x(k) = \begin{bmatrix} i_d(k), i_q(k), \omega_m(k), \\ i_d\omega_m(k), i_q\omega_m(k), i_d i_q(k), T_l \end{bmatrix} \tag{5}$$

If it is the PMSM is surface mounted, the state variables $i_d i_q(k)$ can be neglected automatically.

2.2. MPc

This subsection briefly introduces the MPC theory [27,28]. The target system is a discrete-time linear time-invariant PMSM:

$$\begin{aligned} x_o(k+1) &= A_o x_o(k) + B_o u(k) \\ y_o(k) &= C_o x_o(k) \end{aligned} \tag{6}$$

Subject to:

$$y_{\min} \leqslant y_o(k) \leqslant y_{\max}, u_{\min} \leqslant u_o(k) \leqslant u_{\max} \tag{7}$$

where, k is the k-th sampling period; $x_o(k)$ is an n-dimensional state variable vector are the state variable vectors; $u(k)$ is an m-dimensional control variable vector; $y_o(k)$ is a q-dimensional output variable.

To predict the future state of the system, MPC searches for the optimal input control signal that minimizes the cost function of the state variables. Without loss of generality, the cost function can be defined as:

$$\begin{aligned} J(u,x) &= x_o(k+N_p)^T P x_o(k+N_p) \\ &+ \sum_{i=0}^{Np-1} [x_o^T(k+i) Q x_o(k+i) + u(k+i)^T R u(k+i)] \end{aligned} \tag{8}$$

Subject to:

$$\begin{aligned} y_{\min} \leqslant y_o(k) \leqslant y_{\max} \quad & k = 1,\ldots,N_p \\ u_{\min} \leqslant u(k) \leqslant u_{\max} \quad & k = 0,\ldots,N_c \\ u(k_i + j) = K x_o(k_i + j) \quad & N_c \leqslant j \leqslant N_p \\ x_o(k_i + j + 1) = A_o x(k_i + j) + B_o u(k_i + j) & \\ 0 \leqslant j \leqslant N_p - 1 & \end{aligned} \tag{9}$$

where, N_p and N_c are the predictive and control horizon lengths, respectively; Q, R, and P are the weighting matrices of the current, input, and final states, respectively.

The following can be derived from the first formula in set (6):

$$\begin{aligned} x_o(k_i+1) &= A_o x_o(k_i) + B_o u(k_i) \\ x_o(k_i+2) &= A_o^2 x(k_i) + A_o B_o u(k_i) + B_o u(k_i) \\ x_o(k_i+j) &= A_o^j x_o(k_i) + \sum_{i=0}^{j-1} A_o^i B_o u(k_i + j - 1 - i) \end{aligned} \tag{10}$$

Substituting (10) into (8) and (9):

$$\begin{aligned} y_o(k_i+j) &= C_o \Omega x_o(k_i+j) + C_o \tau u(k_i+j) \\ J[u,x] &= x_o(k_i+j)^T (Q + \Omega^T P \Omega) \\ &+ u(k_i+j)^T (\tau^T P \tau + R) u(k_i+j) \\ &+ 2 x_o(k_i+j)^T \Omega^T P \tau u(k_i+j) \end{aligned} \tag{11}$$

where

$$\Omega = \begin{bmatrix} A_o \\ A_o^2 \\ \ldots \\ A_o^{N_p} \end{bmatrix}, \tau = \begin{bmatrix} B_o & 0 & \ldots & 0 \\ A_o B_o & B_o & \ldots & 0 \\ \ldots & \ldots & \ldots & 0 \\ A_o^{N_p-1} B_o & A_o^{N_p-2} B_o & \ldots & B_o \end{bmatrix} \tag{12}$$

For readability, the following symbols were introduced:

$$\begin{aligned} Y &= 2(Q + \Omega^T P \Omega) \\ H &= 2(\tau^T P \tau + R) \\ F &= \Omega^T P \tau \\ E &= C_o \Omega \\ G &= C_o \tau \end{aligned} \tag{13}$$

Through the above transform, the cost function can be converted into:

$$J[u,x] = \frac{1}{2} x^T(k) Y x(k) + \frac{1}{2} u^T H u + x_k^T F u \tag{14}$$

Subject to

$$Ex(k) + Gu \leqslant W \tag{15}$$

Now, the MPC becomes a multiparametric quadratic programming problem (MPQP). The optimal solution of the problem can be found with modern control theories.

2.3. Laguerre functions

The Laguerre functions in the z-domain can be specified as [29,30]:

$$\begin{aligned} L_N(z) &= \frac{\sqrt{1-a^2}}{1-az^{-1}} \left(\frac{z^{-1}-a}{1-az^{-1}}\right)^{N-1} \\ &= L_{N-1}(z) \frac{z^{-1}-a}{1-az^{-1}} \end{aligned} \tag{16}$$

where, a $\in$ [0, 1] is the time scale factor. This user-defined factor can regulate the system stability [26].

Another version of Laguerre functions in time domain with inverse z-transform can be expressed as:

$$\begin{aligned} L(k+1) &= A_l L(k) \\ L(k) &= \{l_1(k), l_2(k) \ldots l_N(k)\} \end{aligned} \tag{17}$$

where

$$\beta = \sqrt{1-a^2}$$

$$A_l = \begin{bmatrix} a & 0 & \ldots & 0 & 0 \\ \beta & a & \ldots & 0 & 0 \\ -a\beta & \beta & \ldots & 0 & 0 \\ a^2\beta & -a\beta & \ldots & 0 & 0 \\ \ldots & \ldots & \ldots & \ldots & \ldots \\ (-1)^{N-2} a^{N-2} & (-1)^{N-3} a^{N-3} & \ldots & \beta & a \end{bmatrix} \tag{18}$$

It is well known that the impulse response of a linear system can be expressed through discrete Laguerre expansion:

$$h(k) = \sum_{i=1}^{\infty} c_i l_i(k) \tag{19}$$

where, c_i is the Laguerre coefficient.

Taking the differences of control variables between adjacent sampling periods as the impulse response of a stable system, u in (6) was replaced with _u to produce the augmented model, i.e., new state equations [31]:

$$\begin{aligned} x(k+1) = \begin{bmatrix} \Delta x_o(k+1) \\ y(k+1) \end{bmatrix}, A = \begin{bmatrix} A_o & O_o^T \\ C_o A_o & 1 \end{bmatrix} \\ B = \begin{bmatrix} B_o \\ C_o B_o \end{bmatrix}, C = [O_o \quad 1] \end{aligned} \tag{20}$$

where

$$x(k+1)=\begin{bmatrix}\Delta x_o(k+1)\\ y(k+1)\end{bmatrix},A=\begin{bmatrix}A_o & O_o^T\\ C_oA_o & 1\end{bmatrix}$$
$$B=\begin{bmatrix}B_o\\ C_oB_o\end{bmatrix},C=[O_o \quad 1] \tag{21}$$

Let k_i be the initial sampling period, and j be the future sampling period. Substituting the Laguerre expansion (19) into model (20), the new state equations can be obtained [31]:

$$\begin{aligned}x(k_i+j)&=A^jx(k_i)+\sum_{l=0}^{j-1}A_{j-l-1}BL(l)^T\eta\\ y(k_i+j)&=CA^jx(k_i)+\sum_{l=0}^{j-1}CA_{j-l-1}BL(l)^T\eta\end{aligned} \tag{22}$$

where, η is the Laguerre function coefficient vector, containing N c_i values [26]:

$$\eta=[c_1,c_2,...,c_N]^T \tag{23}$$

Substituting (22) into the cost function (14) and its constraints (15) and neglecting the terminal term [26]:

$$J=\eta^T(\sum_{j=1}^{Np}\phi(j)Q\phi(j)^T+R_L)\eta+2\eta^T(\sum_{j=1}^{Np}\phi(j)QA^j)x(k_i) \tag{24}$$

Subject to:

$$M\eta\leqslant b \tag{25}$$

where $\phi(j)^T=\sum_{i=0}^{j-1}A^{j-i-1}BL(i)^T$; M and b are constraints matrices of η.

3. LMPC-Based PMSM control

In this section, the original PMSM model is replaced with the augmented model, and controlled by the algorithm of Laguerre functions in MPC (LMPC).

3.1. Augmented PMSM model

As mentioned in Section 2, the original state variables can be selected as:

$$x_o(k)=\begin{bmatrix}i_d(k),i_q(k),\omega_m(k),\\ i_d\omega_m(k),i_q\omega_m(k),i_di_q(k)\end{bmatrix} \tag{26}$$

To track the PMSM performance, the currents of axis d and q, as well as speed were added to the output variables:

$$y_o(k)=\left[i_d(k),i_q(k),\omega_m(k)\right]^T \tag{27}$$

Thus, the coefficient matrix (A_o,B_o,C_o) of variables (26) (27) can be obtained:

$$B_o=\begin{bmatrix}\frac{T}{L_d} & 0 & 0 & 0 & 0 & 0\\ 0 & \frac{T}{L_q} & 0 & 0 & 0 & 0\end{bmatrix}$$
$$C_o=\begin{bmatrix}1&0&0&0&0&0&0\\0&1&0&0&0&0&0\\0&0&1&0&0&0&0\end{bmatrix}$$
$$A_o=\begin{bmatrix}\frac{L_d-TR_s}{L_d} & 0 & 0 & 0 & \frac{TPL_q}{L_d} & 0 & 0\\ 0 & \frac{L_q-TR_s}{L_q} & -\frac{TP\phi_f}{L_q} & -\frac{TPL_d}{L_q} & 0 & 0 & 0\\ 0 & \frac{1.5TP\phi_f}{J} & \frac{BT+J}{J} & 0 & 0 & \frac{1.5TP(L_d-L_q)}{J} & -\frac{T}{J}\\ 0&0&0&1&0&0&0\\0&0&0&0&1&0&0\\0&0&0&0&0&1&0\\0&0&0&0&0&0&1\end{bmatrix} \tag{28}$$

According to the theory of Laguerre functions, the augmented model of (26) can be derived:

$$x(k)=\begin{bmatrix}\Delta i_d(k),\Delta i_q(k),\\ \Delta\omega_m(k),\Delta i_d\omega_m(k),\Delta i_q\omega_m(k),\\ \Delta i_di_q(k),\Delta T_l,i_d(k),i_q(k),\omega_m(k)\end{bmatrix}$$
$$y(k)=[i_d(k),i_q(k),\omega_m(k)] \tag{29}$$

$$B=\begin{bmatrix}\frac{T}{L_d} & 0&0&0&0&0&0&\frac{T}{L_d}&0&0\\ 0&\frac{T}{L_q}&0&0&0&0&0&\frac{T}{L_q}&0\end{bmatrix}^T$$
$$C=\begin{bmatrix}0&0&0&0&0&0&0&1&0&0\\0&0&0&0&0&0&0&0&1&0\\0&0&0&0&0&0&0&0&0&1\end{bmatrix}$$
$$A=\begin{bmatrix}\frac{L_d-TR_s}{L_d} & 0 & 0 & 0 & \frac{TPL_q}{L_d} & 0 & 0&0&0&0\\ 0 & \frac{L_q-TR_s}{L_q} & -\frac{TP\phi_f}{L_q} & -\frac{TPL_d}{L_q} & 0 & 0 & 0&0&0&0\\ 0 & \frac{1.5TP\phi_f}{J} & \frac{BT+J}{J} & 0 & 0 & \frac{1.5TP(L_d-L_q)}{J} & -\frac{T}{J}&0&0&0\\ 0&0&0&1&0&0&0&0&0&0\\0&0&0&0&1&0&0&0&0&0\\0&0&0&0&0&1&0&0&0&0\\0&0&0&0&0&0&1&0&0&0\\ \frac{L_d-TR_s}{L_d} & 0 & 0 & 0 & \frac{TPL_q}{L_d} & 0 & 0&1&0&0\\ 0 & \frac{L_q-TR_s}{L_q} & -\frac{TP\phi_f}{L_q} & -\frac{TPL_d}{L_q} & 0 & 0 & 0&0&1&0\\ 0 & \frac{1.5TP\phi_f}{J} & \frac{BT+J}{J} & 0 & 0 & -\frac{1.5TP(L_d-L_q)}{J} & -\frac{T}{J}&0&0&1\end{bmatrix} \tag{30}$$

3.2. Laguerre-based MPC on PMSM

The PMSM is an asymptotical system. Once the system is stabilized, the differences of control variables Δu_d and Δu_q between adjacent sampling periods will become zero after a few sampling periods. Therefore, the difference of control variables can be regarded as the impulse response of a stable dynamic system, and described by a set of Laguerre functions according to prior knowledge:

$$\begin{aligned}\Delta u(k_i+j) &= \begin{bmatrix} u_d(k_i+j) \\ u_q(k_i+j) \end{bmatrix} \\ eqalign &= \begin{bmatrix} L_{ud}(j) & 0 \\ 0 & L_{uq}(j) \end{bmatrix} \begin{bmatrix} \eta_{ud} \\ \eta_{uq} \end{bmatrix} \\ &= L(j)^T \eta \end{aligned} \tag{31}$$

And

$$\begin{aligned} L(j)^T &= \begin{bmatrix} l_1^{ud}(j) & \dots & l_{N_i}^{ud}(j) & 0 & 0 & 0 \\ 0 & 0 & 0 & l_1^{uq}(j) & \dots & l_{N_j}^{uq}(j) \end{bmatrix} \\ \eta &= \begin{bmatrix} c_1^{ud} & \dots & c_{N_i}^{ud} & c_1^{uq} & \dots & c_{N_j}^{uq} \end{bmatrix}^T \end{aligned} \tag{32}$$

where, k_i is the current sampling period; j is the j-th sampling period; N_i and N_j are the number of Laguerre coefficients of Δu_d and Δu_q, respectively.

Besides the PMSM Model, a proper cost function is also needed to optimize control variables. Taking (24) as the state weighting matrix, the following control variable weighting matrix can be designed to improve the PMSM performance:

$$Q = C^T \begin{bmatrix} 1.2 & 0 & 0 \\ 0 & 1.2 & 0 \\ 0 & 0 & 1000000 \end{bmatrix} C, R_L = \begin{bmatrix} 0.1 & 0 \\ 0 & 0.1 \end{bmatrix} \tag{33}$$

Fig. 1 shows the voltage of d- and q-axis. In (a), using the algorithm of LMPC with Np = 5, a1 = a2 = 0.5, N1 = N2 = 4. In (b), using the algorithm of MPC with Np = 55. Let the PMSM running from 0 to 100 rad/s with load 4Nm, the voltage under LMPC fluctuates during the starting phase, while at the steady phase, the difference of voltage between LMPC and MPC are small. So, the voltage can be approximate by Laguerre function but with smaller predictive number.

It is also important to ascertain the constraints of state, input, and output variables of the cost function. It is well known that the stator voltage and stator current of PMSM must respectively satisfy the voltage circle and current circle:

$$\begin{aligned} u_d^2 + u_q^2 &\leqslant U_{max}^2 \\ i_d^2 + i_q^2 &\leqslant I_{max}^2 \end{aligned} \tag{34}$$

The two linear constraints above cannot be directly used. Through space vector pulse width modulation (SVPWM), the voltage and current constraints can be approximated in linear form [4]:

$$\begin{bmatrix} -1 & -\frac{1}{\sqrt{3}} \\ -1 & \frac{1}{\sqrt{3}} \\ 0 & \frac{2}{\sqrt{3}} \\ 0 & -\frac{2}{\sqrt{3}} \\ 1 & -\frac{1}{\sqrt{3}} \\ 1 & -\frac{1}{\sqrt{3}} \end{bmatrix} \begin{bmatrix} u_d(k) \\ u_q(k) \end{bmatrix} \leqslant \begin{bmatrix} u_{\max} \\ u_{\max} \\ u_{\max} \\ u_{\max} \\ u_{\max} \\ u_{\max} \end{bmatrix}, \begin{bmatrix} -\frac{1}{\sqrt{3}} & -1 \\ \frac{1}{\sqrt{3}} & -1 \\ \frac{2}{\sqrt{3}} & 0 \\ -\frac{2}{\sqrt{3}} & 0 \\ -\frac{1}{\sqrt{3}} & 1 \\ \frac{1}{\sqrt{3}} & 1 \end{bmatrix} \begin{bmatrix} i_d(k) \\ i_q(k) \end{bmatrix} \leqslant \begin{bmatrix} i_{\max} \\ i_{\max} \\ i_{\max} \\ i_{\max} \\ i_{\max} \\ i_{\max} \end{bmatrix} \tag{35}$$

For simplicity, the above inequality can be rewritten as vectors:

$$\begin{aligned} M_v \begin{bmatrix} u_d(k) \\ u_q(k) \end{bmatrix} &\leqslant U_{max} \\ M_i \begin{bmatrix} i_d(k) \\ i_q(k) \end{bmatrix} &\leqslant I_{max} \end{aligned} \tag{36}$$

Using (23), (32), and (36), the PMSM constraints can be described as:

$$\begin{aligned} M_v \begin{pmatrix} \sum_{j=0}^{k-1} L_{u_d}^T(j) & 0 \\ 0 & \sum_{j=0}^{k-1} L_{u_q}^T(j) \end{pmatrix} &\leqslant U_{max} - M_v \begin{bmatrix} u_{ud}(k_i) \\ u_{uq}(k_i) \end{bmatrix} \\ M_i MCB \begin{bmatrix} L_{u_d}^T(0) & 0 \\ 0 & L_{u_q}^T(0) \end{bmatrix} &\leqslant I_{max} - M_i MCAx(k_i) \end{aligned} \tag{37}$$

Since i_d, i_q and $\omega_m$were selected as the output variables, and the constraints are only applied on input voltage and current, the constraint variables can be obtained by:

$$M = \begin{bmatrix} 1 & 0 & 0 \\ 0 & 1 & 0 \end{bmatrix} \tag{38}$$

4. Stability analysis

As analyzed in the former section, the model predictive control is also a *multiparametric quadratic program* problem, the using of Laguerre functions in model predictive control will infect the stability of the PMSM system. Fig. 2 shows the poles under different parameters a and N.

Because of the dimension of PMSM system described in (30) is ten, thus, ten poles exist in the map. Among them, four poles located on the unit circle, which represent the constant state variables $\Delta\omega_m i_d(k)$, $\Delta\omega_m i_q(k)$,$\Delta i_q i_d(k)$, *and* $T_l(k)$ at each sample period in PMSM model. Besides, the remaining complex conjugate couples are all located in the unit circle, the smaller a, the position of poles closer to the origin, the system will more stable.

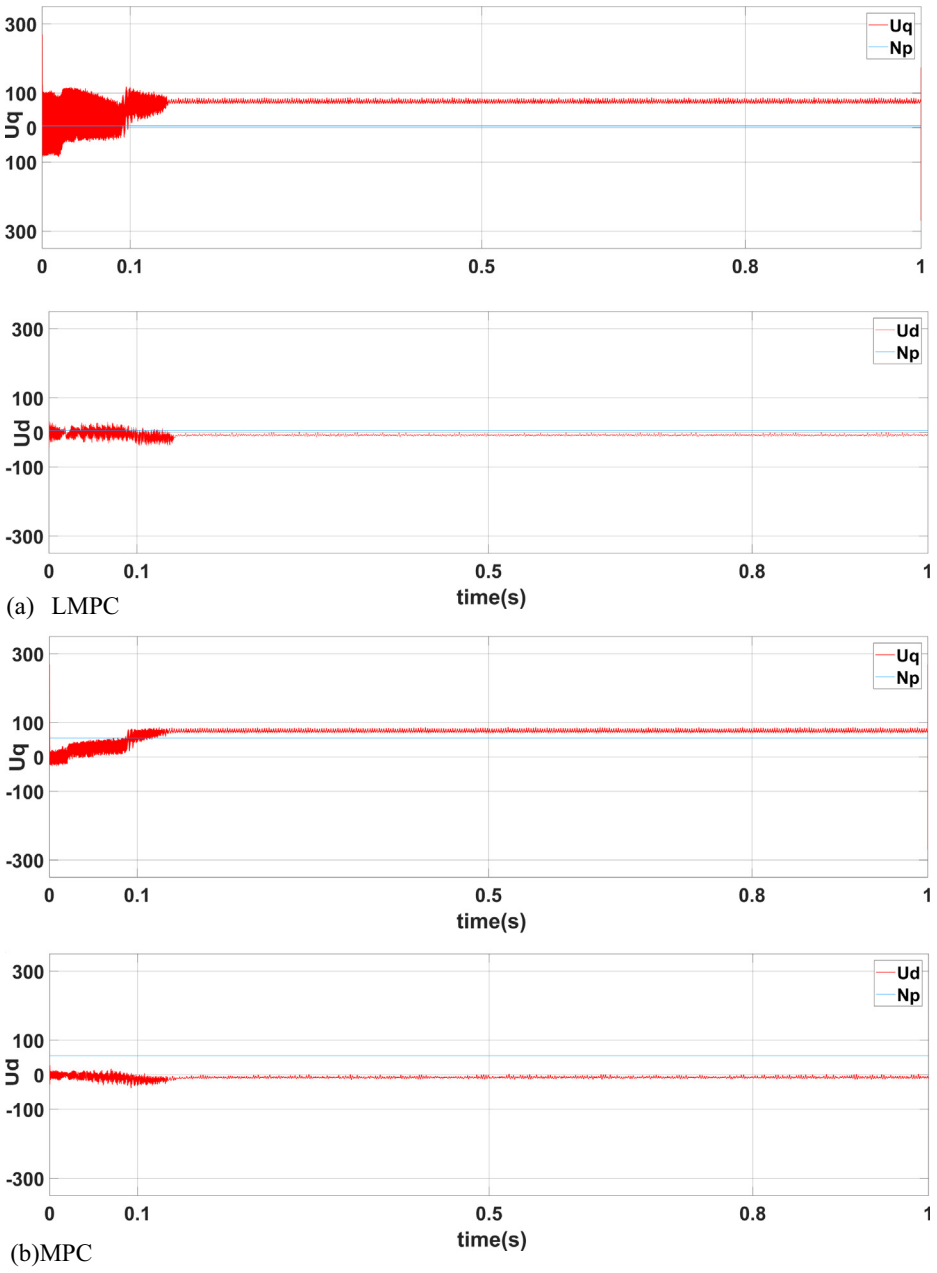

Fig. 1 The voltage based on LMPC and MPC.

5. Result and discussion

To reveal the superiority of LMPC algorithm for PMSM, the LMPC was compared with the MPC without Laguerre functions. Fig. 3 shows the block diagram of LMPC for PMSM. The PMSM parameters are listed in Table 1.

Assuming that the axis d current i_d is zero, two simulations were carried out. During the first simulation, the speed was changed from 0 to 90 rad/s, and a constant load of 4Nm was applied to PMSM at 0.5 s. Then, the PMSM operated at 90 rad/s under the 4Nm load, and controlled by LMPC and MPC, respectively. During the second simulation, the PMSM was controlled by LMPC with different Laguerre parameters. The simulation results are displayed in Figs. 4–8.

5.1. Comparison between LMPC and MPC

(1) Operating efficiency

To verify the efficiency of LMPC, the parameters and results of LMPC and MPC for PMSM are recorded in Table 2. It can be seen that the predictive horizon length N_p of LMPC was set to 4, while that of MPC must be set to 55 to include the most relevant part of system dynamics. The greater length in MPC increases the computing load of the controller.

By MPC, it took 11,281 μs to find the optimal voltage _u in each sampling period. The time consumption was reduced by 437 times with LMPC. Therefore, LMPC can greatly lower the computing load, and apply better to PMSM control.

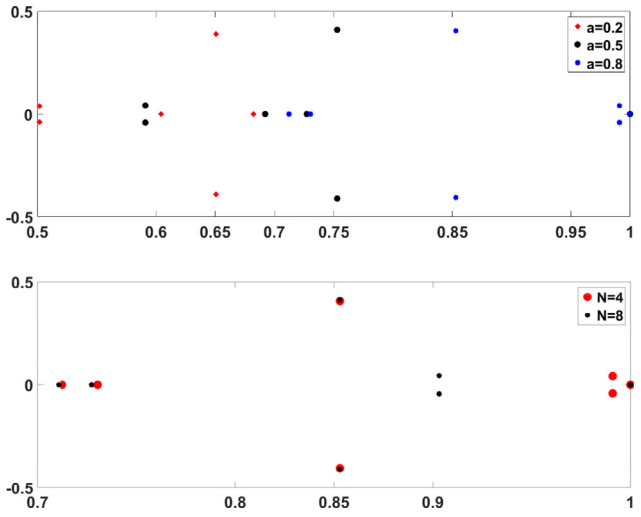

Fig. 2 Pole map under different a and N.

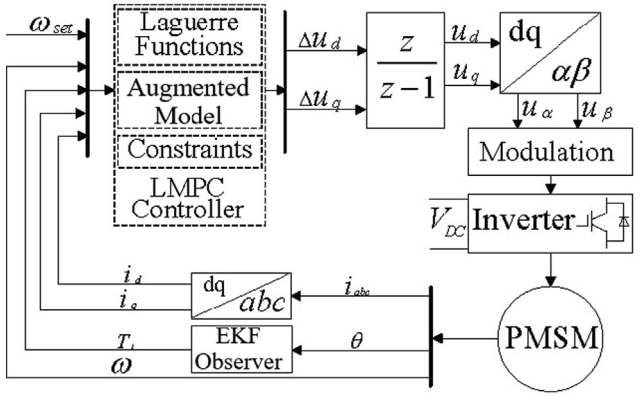

Fig. 3 The block diagram of LMPC for PMSM.

Table 1 The PMSM parameters.

Symbol	Parameter	Value
R_s	Stator resistance	0.9585Ω
L_d	Axis d inductance	0.004987mH
L_q	Axis q inductance	0.005513mH
ϕ_f	Permanent flux linkage	0.1827Wb
P	Number of poles	4
U_{max}	Maximum voltage	171 V
I_{max}	Maximum current	20A
T_s	Sampling periods	0.000005 s

(2) Performance

Figs. 3–5 present the response curves of speed, axis d current, and axis q current under LMPC with $N_p = 4$, $N_c = 2$, $N = 2$, and $a = 0.2$, and MPC with $N_p = 55$ and $N_c = 2$, respectively. It can be seen that, regardless of LMPC or MPC, the speed remained stable after PMSM arrived at the set point, an evidence of good speed response without steady-state error.

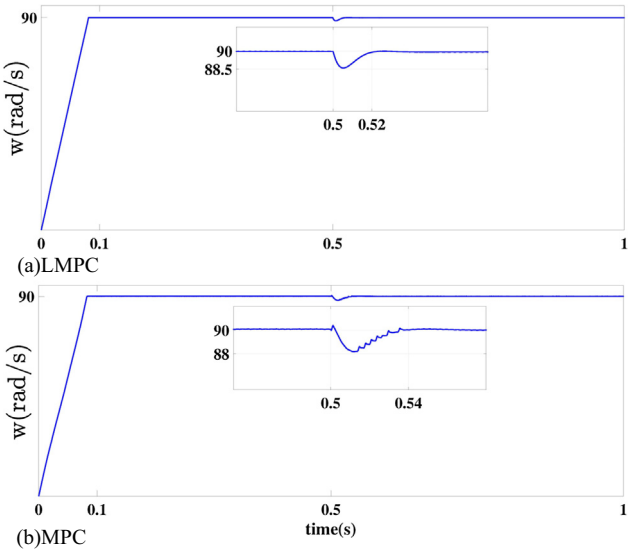

Fig. 4 The speed response curves of LMPC and MPC.

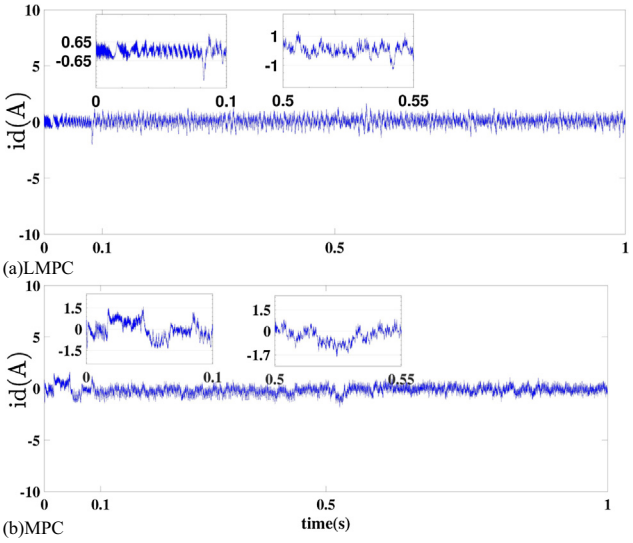

Fig. 5 The current id response curves of LMPC and MPC.

As shown in Fig. 4, LMPC made faster adjustment and achieved smaller speed error than MPC, when the load changed at 0.5 s. As shown in Figs. 5 and 6, the LMPC had a relatively low current overshoot during start-up, while MPC brought a noticeable damped oscillation. This is because the current constraints in LMPC affect axis q current i_q.

To reveal the superiority of LMPC, the speed errors and currents of LMPC and MPC under external load are compared in Tables 3 and 4, respectively.

The above analysis shows that LMPC with N = 2 and a = 0.2 achieved comparable performance as MPC with predictive horizon length $N_p = 55$, while greatly reducing the computing load. This fully demonstrates the excellence of LMPC for PMSM.

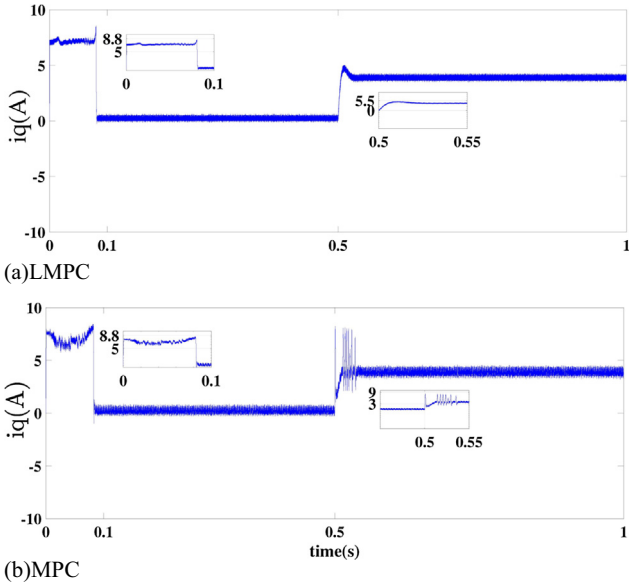

(a)LMPC

(b)MPC

Fig. 6 The current i_q response curves of LMPC and MPC.

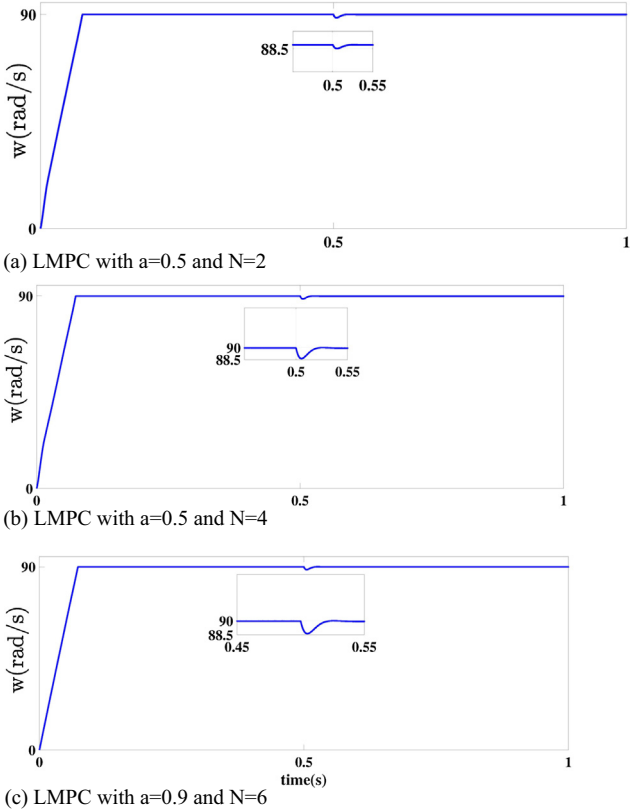

(a) LMPC with a=0.5 and N=2

(b) LMPC with a=0.5 and N=4

(c) LMPC with a=0.9 and N=6

Fig. 7 The speed response curves of LMPC with different Laguerre parameters.

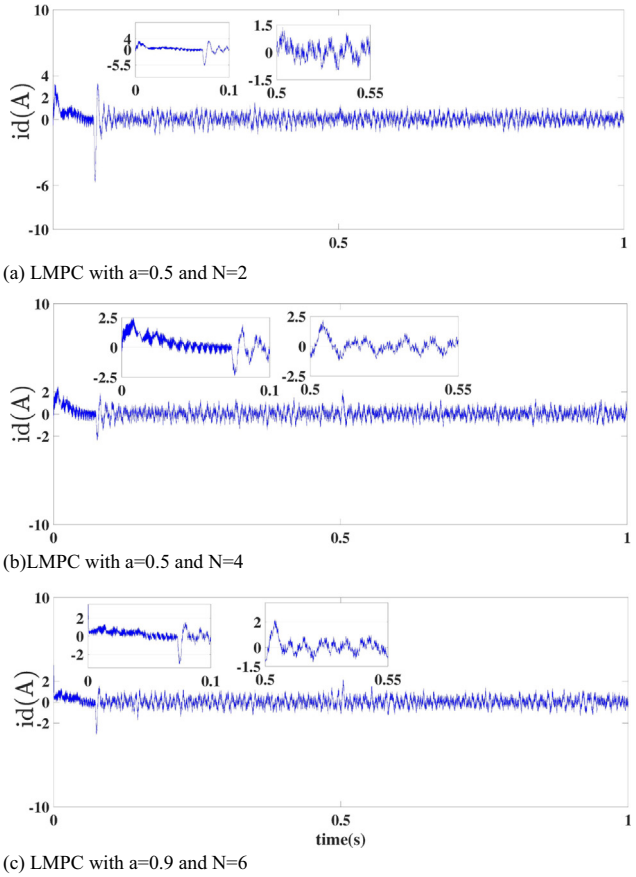

(a) LMPC with a=0.5 and N=2

(b)LMPC with a=0.5 and N=4

(c) LMPC with a=0.9 and N=6

Fig. 8 The current i_d response curves of LMPC with different Laguerre parameters.

Table 3 The comparison of speed error.

Method	Maximum speed error(rad/s)	Time(s)
MPC	2	0.02
LMPC	1.5	0.04

5.2. Comparison between different Laguerre parameters

Table 5 and Figs. 7–9 illustrate the effects of PMSM control by LMPC control algorithms with different a and N values. From these figures, it can be noted that the speed responses were good during start up and loading. The most striking difference lies in the optimization time of control variables (Table 5). The greater the values of N and a, the longer the time it took to find the *optimal control variables in each sampling period.*

Moreover, the parameter change led to significant variation in current responses. Under a = 0.5 and N = 2, the maximum

Table 2 The comparison of operating efficiency.

Method	N_p	N_c	N	a	Time (μs)
MPC	55	5	–	–	11,281
LMPC	4	2	2	0.2	25.8

Table 4 The comparison of current.

Interval(s)	Method	Max i_d (A)	Max i_q (A)
0–0.1	MPC	1.5	8.8
	LMPC	0.65	8.8
0.5–0.6	MPC	1.5	9
	LMPC	1	5.5

Table 5 The comparison of LMPC performance with different Laguerre parameters.

a	N	Time (μs)	Maximum errorof i_d (A)	Maximum errorof i_q (A)
0.2	2	25.8	2	8.5
0.5	2	31.7	6	12
0.5	4	37.2	2	11.5
0.9	6	40	2.3	8.5

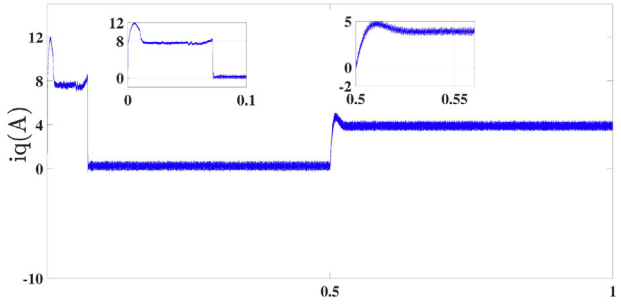

(a) LMPC with a=0.5 and N=2

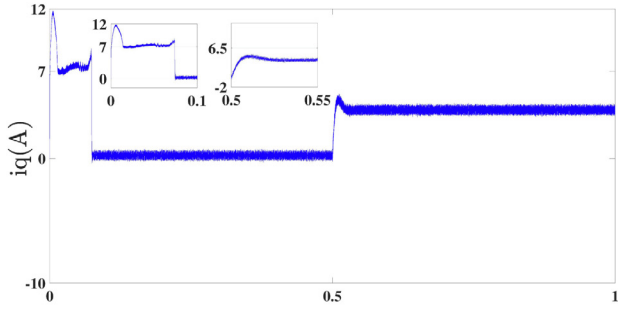

(b) LMPC with a=0.5 and N=4

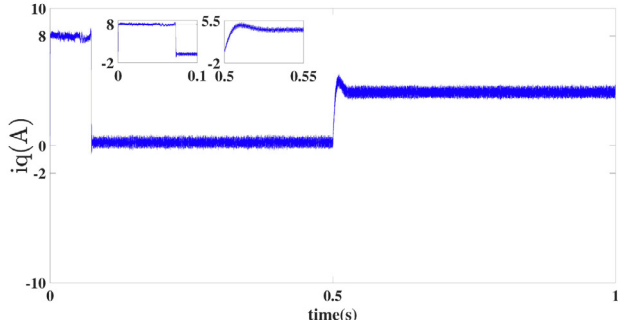

(c) LMPC with a=0.9 and N=6

Fig. 9 The current i_q response curves of LMPC with different Laguerre parameters.

i_q was about 12A; under a = 0.9 and N = 6, the maximum i_q was about 8A. This means the PMSM performance can be regulated by adjusting the parameters of the Laguerre functions.

6. Conclusions

To improve the performance of MPC on PMSM control, this paper proposes a MPC algorithm with Laguerre functions. In the proposed algorithm LMPC, the optimal control variables were resolved by Laguerre functions. And by the adjustment of Laguerre parameter, the convergence speed of increment voltage can be adjusted with shorter predictive control period compared to the MPC. Simulation results confirm that the LMPC has better control performance than MPC. The future research will investigate the impact of changing internal parameters of PMSM on LMPC.

Declaration of Competing Interest

The authors declare that they have no known competing financial interests or personal relationships that could have appeared to influence the work reported in this paper.

References

[1] J.M. Mun, G.J. Park, S. Seo, Y.J. Kim, S.Y. Jung, Design characteristics of IPMSM with wide constant power speed range for EV traction, IEEE Trans. Magn. 53 (6) (2017) 1–4.
[2] C. Liu, K.T. Chau, X. Zhang, An efficient wind–photovoltaic hybrid generation system using doubly excited permanent-magnet brushless machine, IEEE Trans. Ind. Electron. 57 (3) (2009) 831–839.
[3] H. Abdellaoui, K. Ghedamsi, A. Mecharek, Performance and lifetime increase of the PEM fuel cell in hybrid electric vehicle application by using an NPC seven-level inverter, J. Européen des Systèmes Automatisés 52 (3) (2019) 325–332.
[4] N. Bounasla, S. Barkat, Optimum design of fractional order PI[a] speed controller for predictive direct torque control of a sensorless five-phase Permanent Magnet Synchronous Machine (PMSM), J. Européen des Systèmes Automatisés 53 (4) (2020) 437–449.
[5] C. Liu, K.T. Chau, J.Z. Jiang, A permanent-magnet hybrid brushless integrated starter–generator for hybrid electric vehicles, IEEE Trans. Ind. Electron. 57 (12) (2010) 4055–4064.
[6] A. Chenna, D. Aouzellag, K. Ghedamsi, Study and control of a pumped storage hydropower system dedicated to renewable energy resources, J. Européen des Systèmes Automatisés 53 (1) (2020) 95–102.
[7] J. Liu, C. Gong, Z. Han, H. Yu, IPMSM model predictive control in flux-weakening operation using an improved algorithm, IEEE Trans. Ind. Electron. 65 (12) (2018) 9378–9387.
[8] Z. Mynar, L. Vesely, P. Vaclavek, PMSM model predictive control with field-weakening implementation, IEEE Trans. Ind. Electron. 63 (8) (2016) 5156–5166.
[9] F. Niu, B. Wang, A.S. Babel, K. Li, E.G. Strangas, Comparative evaluation of direct torque control strategies for permanent magnet synchronous machines, IEEE Trans. Power Electron. 31 (2) (2015) 1408–1424.
[10] G. Chandaka, G. Prasanth, Direct torque control and field oriented control of PMSM using SVPWM Technique, Int. J. Adv. Res. Sci. Eng 3 (11) (2014).
[11] C.S. Lim, E. Levi, M. Jones, N.A. Rahim, W.P. Hew, A comparative study of synchronous current control schemes

based on FCS-MPC and PI-PWM for a two-motor three-phase drive, IEEE Trans. Ind. Electron. 61 (8) (2013) 3867–3878.
[12] A.E.H.M. Elbeltagy, A.M. Youssef, A.M. Bayoumy, Y.Z. Elhalwagy, Fixed ground-target tracking control of satellites using a nonlinear model predictive control, Math. Model. Eng. Problems 5 (1) (2018) 11–20.
[13] J.D. Barros, J.F.A. Silva, É.G. Jesus, Fast-predictive optimal control of NPC multilevel converters, IEEE Trans. Ind. Electron. 60 (2) (2012) 619–627.
[14] T. Geyer, G. Papafotiou, M. Morari, Model predictive direct torque control—Part I: Concept, algorithm, and analysis, IEEE Trans. Ind. Electron. 56 (6) (2008) 1894–1905.
[15] L. Danza, L. Belussi, F. Floreani, I. Meroni, A. Piccinini, F. Salamone, Application of model predictive control for the optimization of thermo-hygrometric comfort and energy consumption of buildings, Instrum. Mesure Métrologie 17 (3) (2018) 375–391.
[16] S. Ding, J.H. Park, C.C. Chen, Second-order sliding mode controller design with output constraint, Automatica 112 (2020) 108704.
[17] J. Rodriguez, J. Pontt, C.A. Silva, P. Correa, P. Lezana, P. Cortés, U. Ammann, Predictive current control of a voltage source inverter, IEEE Trans. Ind. Electron. 54 (1) (2007) 495–503.
[18] Y. Luo, C. Liu, F. Yu, Predictive current control of a new three-phase voltage source inverter with phase shift compensation, IET Electr. Power Appl. 11 (5) (2017) 740–748.
[19] S. Vazquez, J. Rodriguez, M. Rivera, L.G. Franquelo, M. Norambuena, Model predictive control for power converters and drives: advances and trends, IEEE Trans. Ind. Electron. 64 (2) (2016) 935–947.
[20] Y. Zhang, H. Yang, Two-vector-based model predictive torque control without weighting factors for induction motor drives, IEEE Trans. Power Electron. 31 (2) (2015) 1381–1390.
[21] C.E. Garcia, D.M. Prett, M. Morari, Model predictive control: theory and practice—a survey, Automatica 25 (3) (1989) 335–348.
[22] D.Q. Mayne, J.B. Rawlings, C.V. Rao, P.O. Scokaert, Constrained model predictive control: Stability and optimality, Automatica 36 (6) (2000) 789–814.
[23] M. Preindl, S. Bolognani, Model predictive direct torque control with finite control set for PMSM drive systems, part 2: Field weakening operation, IEEE Trans. Ind. Inf. 9 (2) (2012) 648–657.
[24] S. Bolognani, S. Bolognani, L. Peretti, M. Zigliotto, Design and implementation of model predictive control for electrical motor drives, IEEE Trans. Ind. Electron. 56 (6) (2008) 1925–1936.
[25] C. Hwang, K.K. Shyu, Analysis and identification of discrete-time systems via discrete Laguerre functions, Int. J. Syst. Sci. 18 (10) (1987) 1815–1824.
[26] L. Wang, Discrete model predictive controller design using Laguerre functions, J. Process Control 14 (2) (2004) 131–142.
[27] A. Bemporad, M. Morari, V. Dua, E.N. Pistikopoulos, The explicit solution of model predictive control via multiparametric quadratic programming, in: Proceedings of the 2000 American Control Conference. ACC (IEEE Cat. No. 00CH36334), 2, 2000, June, pp. 872–876.
[28] S. Hovland, K. Willcox, J.T. Gravdahl, MPC for large-scale systems via model reduction and multiparametric quadratic programming, in: Proceedings of the 45th IEEE Conference on Decision and Control, 2006, pp. 3418–3423.
[29] Y. Fu, G.A. Dumont, An optimum time scale for discrete Laguerre network, IEEE Trans. Autom. Control 38 (6) (1993) 934–938.
[30] B. Maione, B. Turchiano, Laguerre z-transfer function representation of linear discrete-time systems, Int. J. Control 41 (1) (1985) 245–257.
[31] L. Wang, Model Predictive Control System Design and Implementation using MATLAB®, Springer Science & Business Media, 2009.